Article

Modulation of the Singlet Oxygen Generation from the Double Strand DNA-SYBR Green I Complex Mediated by T-Melamine-T Mismatch for Visual Detection of Melamine

Hao Hu, Jinyi Zhang, Yu Ding, Xinfeng Zhang, Kailai Xu, Xiandeng Hou, and Peng Wu

Anal. Chem., **Just Accepted Manuscript** • DOI: 10.1021/acs.analchem.7b00666 • Publication Date (Web): 06 Apr 2017

Modulation of the Singlet Oxygen Generation from the Double Strand DNA-SYBR Green I Complex Mediated by T-Melamine-T Mismatch for Visual Detection of Melamine

Hao Hu,[†] Jinyi Zhang,[‡] Yu Ding,[†] Xinfeng Zhang,[‖] Kailai Xu,[‡,*] Xiandeng Hou,[†, ‡] Peng Wu[†, ‡, *]

[†]Analytical & Testing Center, and [‡]College of Chemistry, Sichuan University, 29 Wangjiang Road, Chengdu 610064, China

[‖]College of Materials and Chemistry & Chemical Engineering, Chengdu University of Technology, Chengdu 610059, China

*Corresponding authors: wupeng@scu.edu.cn (PW), xukailai@scu.edu.cn (KX)

ABSTRACT

Singlet oxygen ($^1O_2$), generated via photosensitization, has been proved to oxidize chromogenic substrates with neither H_2O_2 oxidation nor enzyme (horseradish peroxidase, HRP) catalysis. Of the various methods for modulation of the $^1O_2$ generation, DNA-controlled photosensitization received great attention. Therefore, integration of the formation/deformation DNA structures with DNA-controlled photosensitization will be extremely appealing in visual biosensor developments. Here, the stable melamine-thymine complex was explored in combination with DNA-controlled photosensitization for visual detection of melamine. A T-rich single stand DNA was utilized as the recognition unit. Upon the formation of T-M-T complex, double stand DNA was formed, which was ready for the binding of SYBR green I and activated the photosensitization. Subsequent oxidation of TMB allowed visual detection of melamine in dairy products, with spike-recoveries ranging from 94% to 106%.

INTRODUCTION

Singlet oxygen ($^1O_2$), generated via photosensitization, is always at the forefront of photochemical and photobiological research.[1] The diverse applications of $^1O_2$ range from materials science to medicine, with particular focus on photodynamic therapy (PDT)[2-3] and water remediation.[4-5] On the other hand, the discovery of new $^1O_2$-involved oxidizing reactions is also on the way. For example, recently it was found that $^1O_2$ could directly oxidize chromogenic substrates (e.g., 3,3',5,5'-tetramethylbenzidine, TMB) with neither H_2O_2 oxidation nor enzyme catalysis,[6-8] opening new avenue for the development of bioassays based on the modulation of photosensitization.

Of the various methods for modulation of the $^1O_2$ generation, DNA-controlled photosensitization received great attention.[9-10] For example, the Gothelf group first demonstrated that the production of $^1O_2$ could be controlled by designed DNA systems (bearing photosensitizer-quencher pair) and thereby turned on by the presence of specific DNA.[11] On the basis of such idea, aptamer[12-14] and mRNA[15] were also explored as input for switching the $^1O_2$ generation. Hirakawa *et al.*, on the other hand, explored the microenvironment of double stand DNA (dsDNA) for activation of the $^1O_2$ production from DNA-binding photosensitizers.[16-19] In addition to the above DNA structures based on the classical Watson-Crick base-pairing, several new DNA structures, such as i-motif[20] and G-quadruplex,[21] are also demonstrated to be effective in modulation of the $^1O_2$ generation. Considering the versatility of various DNA switches[22] and functional DNAs,[23] integration of the formation/deformation DNA

structures with DNA-controlled photosensitization will be extremely appealing in biosensor developments.

Melamine (M) is a low toxicant industrial raw materials to product melamine formaldehyde resin (MF). However, it is illegally added to milk products to increase total nitrogen content of dairy products,[24-27] which can induce humans renal pathology and even death (especially the newborns).[28-32] It has been reported that melamine could form stable triple hydrogen-bonding with thymine (T-M-T).[33] Therefore, we conjectured whether such melamine-thymine complex can be explored in DNA-controlled $^1O_2$ production to combine with $^1O_2$-induced facile oxidation of TMB for visual detection of melamine. To our delight, melamine could indeed mediate the formation of dsDNA from a full T-single strand DNA (ssDNA), which could subsequently capture SYBR green I to switch on its photosensitization (Figure 1A). In combination with the $^1O_2$-induced TMB oxidation,[6-8] a visual biosensor for melamine was constructed.

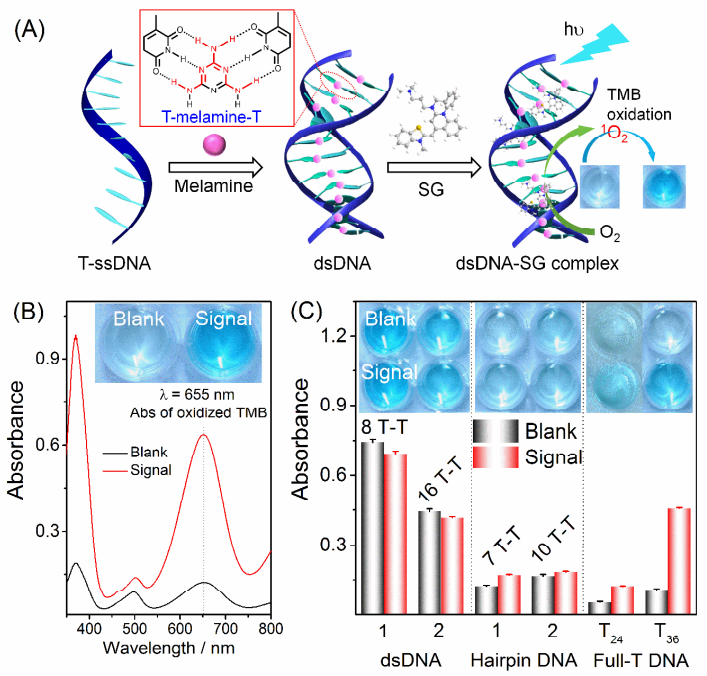

Figure 1 (A) Schematic illustration of the T-M-T-mediated formation of dsDNA and subsequent DNA-controlled photosensitization (SYBR green I, SG) for visual detection of melamine; (B) absorbance profile of TMB upon photosensitized oxidation in the absence (blank) and presence (signal) of dsDNA-SG complex; and (C) effects of different T-rich DNA sequence on the photosensitized oxidation of TMB. The nomination of the DNAs in (C) was according to Table 1. Experimental conditions: DNA, 100 nM; SG, 3.92 μM; melamine, 50 μM; citrate buffer, pH 4.5; and cyan LED.

EXPERIMENTAL SECTION

Materials. 3,3',5,5'-Tetramethylbenzidine (TMB), citrate, disodium hydrogen phosphate, melamine, mannite, catalase, tryptophan, superoxide dismutase (SOD) ascorbic acid, vitamin B, lactose, glucose, cyanuric acid and horseradish peroxidase (HRP) were from Aladdin (Shanghai, China). Sodium hydroxide, hydrochloric acid, hydrogen peroxide (H_2O_2), acetocaustin, and dimethyl sulfoxide (DMSO) were purchased from Kelong Reagent Co. (Chengdu, China). SYBR Grenn I (SG, 10000×)

and singlet oxygen sensor green (SOSG, 100 μg) were from ThermoFisher Scientific (American). The concentration of 10000× SG solution is calculated to be 19.6 mM according to the research from Vitzthum et al.[34] Oligonucleotides were provided by Shanghai Sangon Biotech Co., Ltd. (Shanghai, China, Table 1). Pure milk and milk powder were collected from local supermarket.

Table 1. The Sequences of the Used DNAs in This Work (the T-T mismatches in dsDNA and hairpin were underlined).

Type	Sequence
dsDNA-1 (8 T-T)	5'-CGC ATT CAG GAT TCT CTA CTC GTA-3'
	3'-GCG TTT GTC CTT TGT GTT GTG CTT-5'
dsDNA-2 (16 T-T)	5'-TTC TTC TTC TTC TTC TTC TTC TTC-3'
	3'-TTG TTG TTG TTG TTG TTG TTG TTG-5'
Hairpin-1 (7 T-T)	5'-CTT CTT TCT TCC CCT TGT TTG TTG-3'
Hairpin-2 (10 T-T)	5'-CTT TCT TCT TTC TTC CCC TTG TTT GTT GTT TG-3'
T_{12}	5'-TTTTTTTTTTTT-3'
T_{24}	5'-TTTTTTTTTTTTTTTTTTTTTTTT-3'
T_{36}	5'-TTTTTTTTTTTTTTTTTTTTTTTTTTTTTTTTTTTT-3'
T_{48}	5'-TTTTTTTTTTTTTTTTTTTTTTTTTTTTTTTTTTTTTTTTTTTTTTTT-3'

Apparatus. The UV-Vis absorption spectra, the fluorescence (FL) spectra and the CD spectra were obtained with a UV-1750 spectrophotometer (Shimadzu, Japan), an F-7000 fluorescence spectrophotometer (Hitachi, Japan) and an CD-250 Chirascan-plus spectrophotometer (Applied Photophysics Limited, UK), respectively. The images were taken with a Nikon D300S digital camera equipping a Nikon AF-S VR 105 mm f/2.8G IF-ED Macro Lens without any filters. The Irradiancy of LED

was detected with a FZ-A radiometer (The photoelectric instrument factory of Beijing normal university, China)

Methods. To obtain a typical photocatalytic system, oligothymidine (dT_{36}) DNA, melamine and SG were mixed and diluted to 2 mL with citrate buffer (pH 4.5). The final concentrations of dT_{36} DNA and SG are 100 nM and 3.92 μM (2×), respectively. The mixture was incubated for 20 min, then add TMB irradiated with blue LED for another 10 min.

Sample preparation. For pure milk, 2 mL of homogenized sample was placed into a 10 mL PE tube and 0.15 mL of 300 g/L of trichloroacetic acid aqueous solution was added and mixed with a vortex for 1 min. The mixture was sonicated in an ultrasonic bath for 15 min at room temperature to extract melamine. After stewing for a moment, the mixture was completely filtered into another EP tube. 3 M NaOH was added to adjust the pH to 7, then the extraction was filtered with 0.22 mm filter for detection. For milk powder, 0.4 g of homogenized sample was weighed into a 10 mL PE tube and 2 mL of deionized water was added into the sample. After the sample dissolved, 0.18 mL of 300 g/L of trichloroacetic acid aqueous solution was added. Other steps were the same as above.

RESULTS AND DISCUSSIONS

Design and Validation of Melamine-Mediated Formation of the dsDNA-SYBR Green I Complex for Photosensitized Oxidation of TMB. The design of the melamine-mediated formation of dsDNA complex for switching on the

photosensitization of SYBR green I (SG) was schematically illustrated in Figure 1A. To check the feasibility of the proposed assay, we first designed a T-rich single stand DNA (ssDNA, 36 T bases) as the probe. SYBR green I (SG) was chosen as the photosensitizer because it can bind dsDNA with high affinity.[35] Also, it has already been confirmed that dsDNA-SG complex could generate $^1O_2$ upon photosensitization for TMB oxidation.[8] As is shown in Figure 1B, significantly intensified TMB oxidation was observed in the presence of dsDNA-SG complex (T-M-T-mediated formation of dsDNA) and cyan LED irradiation, indicating enhanced $^1O_2$ generation in such system.[6-8] However, in the absence of the melamine, no dsDNA-SG complex was formed and thus no appreciable TMB oxidation. Therefore, melamine-mediated formation of dsDNA for modulating the $^1O_2$ production was preliminarily confirmed.

To find the optimal probe DNA sequence for melamine detection, several DNA structures were investigated, including dsDNA bearing several T-T mismatches in the middle, hairpin DNA containing several T-T mismatches in the stem,[36] and full T-DNA[33] (Table 1 and Figure S1). As shown in Figure 1C, all these DNAs with melamine could catalyze the oxidation of TMB under cyan LED irradiation, but the full T-DNA (T_{36}) gave the best visual detection performance. Probably, the full T-DNA exhibits the lowest steric hindrance for melamine to be located in, which maximize the difference between ssDNA and dsDNA. For dsDNA-1 (8 T-T) and dsDNA-2 (16 T-T), the blank is almost the same as that of signal. Probably, there is already metastable dsDNA structure for SG binding (as revealed by the SG fluorescence in Figure S2). Insertion of melamine was therefore restricted by the

steric hindrance of the existing dsDNA structure.

The number of thymines in full T-DNA has a remarkable effect on the photosensitization performance. As shown in Figure S3, of the four full T-DNAs (T_{12}, T_{24}, T_{36}, and T_{48}), the signal responses were in the following order: $T_{48} > T_{36} > T_{24} > T_{12}$. Upon comparison of the structure of T-M-T and A-T basepair (Figure S4), it can be seen that longer full T-DNA tends to form more stable dsDNA than shorter ones in the presence of melamine, because of the de-localization of the steric hindrance along the long DNA chain, which is in good accordance with their actual signal responses. Eventually, T_{36}-DNA was chosen since it gave the best signal-to-background ratio for melamine detection.

Confirmation of the Melamine-Mediated Formation of dsDNA. Next, the melamine-mediated formation of dsDNA was experimentally confirmed. Figure 2A shows the absorption spectra of T_{36}-DNA in the absence and presence of melamine. The optical density decreased as melamine introduced, indicating the formation of duplex.[37] Circular dichroism (CD) spectra shows significant structuring of T_{36}-DNA in the presence of melamine, signified by the development of a more positive CD signal at 280 nm (Figure 2B). Therefore, melamine-induced transformation of T_{36}-DNA to dsDNA should be responsible for such structuring.

SG is a famous probe for DNA detection due to its ability to dramatically increase fluorescence brightness upon binding with dsDNA, but not with ssDNA.[35] As shown in Figure 2C and Figure S5, when mixing SG with T_{36}-DNA, the fluorescence of SG was extremely weak. However, in the presence of increasing

amounts of melamine, the fluorescence of SG was gradually increased, indicating that dsDNA was indeed formed from T_{36}-DNA via melamine mediation.

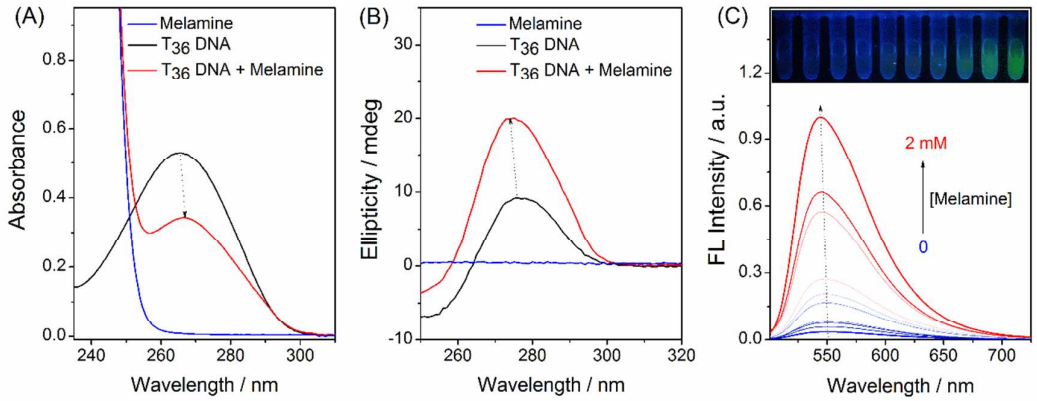

Figure 2 Confirmation of the melamine-mediated formation of dsDNA: (A) UV-vis absorption spectra of melamine, T_{36}-DNA, and T_{36}-DNA-melamine complex; (B) circular dichroism spectra of melamine, T_{36}-DNA, and T_{36}-DNA-melamine complex; and (C) fluorescence spectra of SG in the presence of T_{36}-DNA upon titration with melamine, the inset shows the corresponding fluorescent photos. Experimental conditions: 1 μM T_{36}-DNA and 4 mM melamine for UV-vis and CD; 0.5 μM T_{36}-DNA and 3.92 μM SG for fluorescence; all the spectroscopic investigations were carried in pH 4.5 citrate buffer.

Verification of the Photosensitized Oxidation of TMB. Subsequently, the oxidation of TMB by photosensitization was verified. Photosensitized oxidation occurs first by photon absorption of the sensitizer to trigger the transition from the ground state to the excited state. Therefore, the photosensitization efficiency is directly related to the light absorption. Here, we used LED (3 V, 3 W) as the lighting source. As shown in Figure 3A, the absorption spectrum of SG spans from ~420 nm to ~550 nm, which is overlapped with the lighting wavelength of blue, cyan, and green LEDs. Besides, the cyan LED exhibits largest overlap. Just as expected, the TMB oxidation efficiency was in good accordance with the above spectra overlap order (Figure 3B). Therefore,

cyan LED was selected for illumination.

The LED illumination conditions, including the illumination time, the height of the LED above the micro-well plate, and the irradiance-dependent signal, were studied in detail. As can be seen from Figure S6, illumination time of 10 min, LED height of 3 cm, and LED irradiance of 7.5 mW/cm^2 were selected for the following investigations.

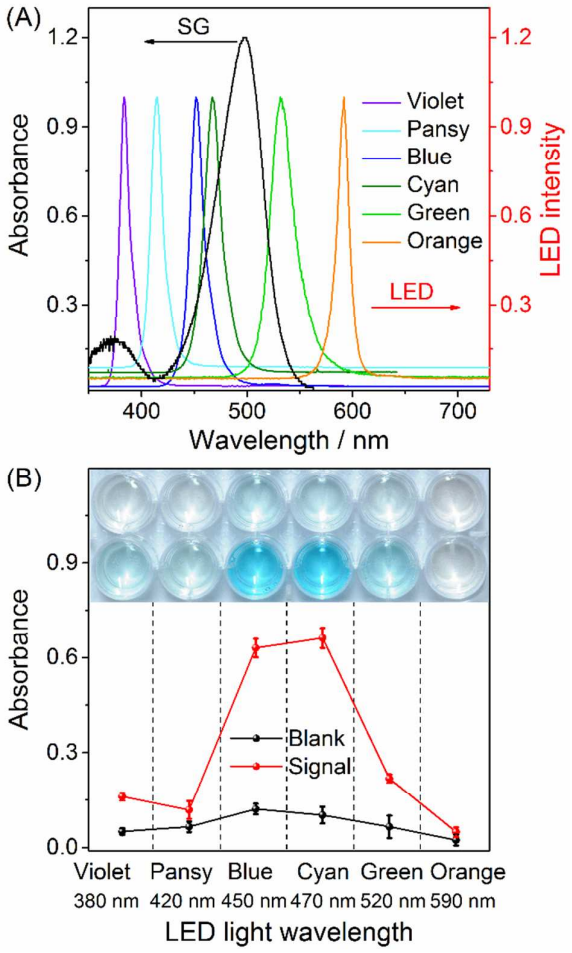

Figure 3 Confirmation of the photosensitized oxidation of TMB: (A) the spectra overlap between the absorption spectrum of SG and lighting wavelength of various LEDs; and (B) TMB oxidation efficiency assisted by violet, pansy, blue, cyan, green, and orange LEDs. Experimental conditions: DNA, 100 nM; SG, 3.92 μM; Melamine, 50 μM; and citrate buffer, pH 4.5.

Photosensitization can generate reaction oxygen species (ROS) through the reduction of molecular oxygen by hydrogen/electron transfer (Type-I) as well as energy transfer from the photoexcited sensitizer (Type-II).[2-3] First, the involvement of O_2 in photosensitized oxidation of TMB was identified. As shown in Figure 4A, the dsDNA (T-M-T)-SG system exhibits highly O_2-dependent photocatalytic oxidation characteristics for TMB, indicating that ROS activated from dissolved O_2 are responsible for the oxidation. To uncover the role of the specific ROS, we used the ROS-specific scavengers to evaluate the contribution of these ROS, namely mannite for ·OH, tryptophan for $^1O_2$, superoxide dismutase (SOD) for $\cdot O_2^-$, and catalase for H_2O_2.[6,38] As shown in Figure 4B, only tryptophan could effectively inhibit the TMB photo-oxidation catalysed by the dsDNA (T-M-T)-SG system, while the other three caused no significant difference, indicating the photosensitized generation of $^1O_2$.

The presence of $^1O_2$ was further verified with the commercial fluorescent capturer Singlet Oxygen Sensor Green (SOSG, Figure S7).[39] As shown in Figure 4C, upon incubating SOSG with the dsDNA (T-M-T)-SG system and irradiating with a cyan LED for 7 min, the fluorescence of SOSG centered at 525 nm was considerably increased. Although the fluorescence of SOSG overlaps with that of SG, control experiments indicated that there was no significant variation of SG fluorescence before and after LED irradiation (Figure 4C). The huge fluorescence increase here could therefore be ascribed to trap of $^1O_2$ by SOSG.

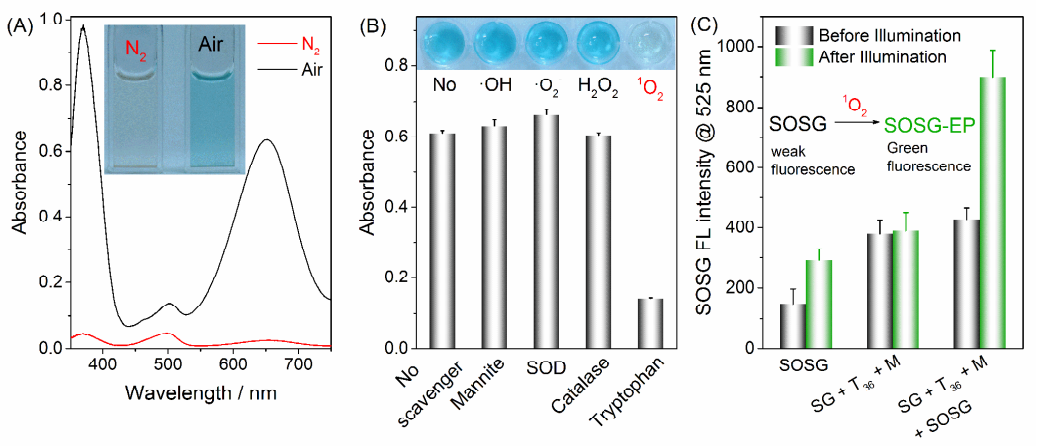

Figure 4 Identification of the specific ROS for TMB oxidation: (A) the effect of dissolved oxygen on TMB photo-oxidation; (B) the use of scavengers for evaluation of the specific ROS in TMB photo-oxidation; and (C) verification of photosensitized generation $^1O_2$ from the dsDNA (T-M-T)-SG system through the commercial commercial fluorescent capturer SOSG. Experimental conditions: DNA, 100 nM; SG, 3.92 μM; melamine, 50 μM; and citrate buffer, pH 4.5. The concentrations of DNA, SG and melamine were enlarged by 2-fold for $^1O_2$ capture in (C).

On the basis of the above evidences, the exact oxidant for TMB oxidation can be identified as $^1O_2$. Again, such evidence also confirmed that melamine-mediated formation of dsDNA from T_{36}-DNA could be explored for modulation the $^1O_2$ generation from DNA-binding photosensitizers.[16-19]

Analytical Performance of This Assay for Melamine Detection. To maximize the sensitivity of the proposed visual assay for melamine, the concentration of T_{36}-DNA and pH of the reaction media were optimized (Figure S8 and S9). Here, citrate buffer (pH = 4.5) was used based on the requirement of the TMB-based colorimetric assay (Figure S9). Under optimal conditions, the absorbance of oxidized TMB increases with the melamine concentration (Figure 5A). A linear correlation (Y = 0.0074C +

0.0145) was obtained between the absorbance of oxidized TMB and the melamine concentration in the range of 0.5-100 μM (R = 0.9906, Figure 5B). The resultant color change allowed visual detection of melamine as low as 0.5 μM (Figure 5B), which is sensitive enough for melamine detection in dairy milk products (Table S1 and Table S2).[40] Compared with fluorescence detection with SG as the probe (Figure 2C), the proposed visual sensor possessed higher sensitivity. Besides, visual detection with naked eye is much simpler.

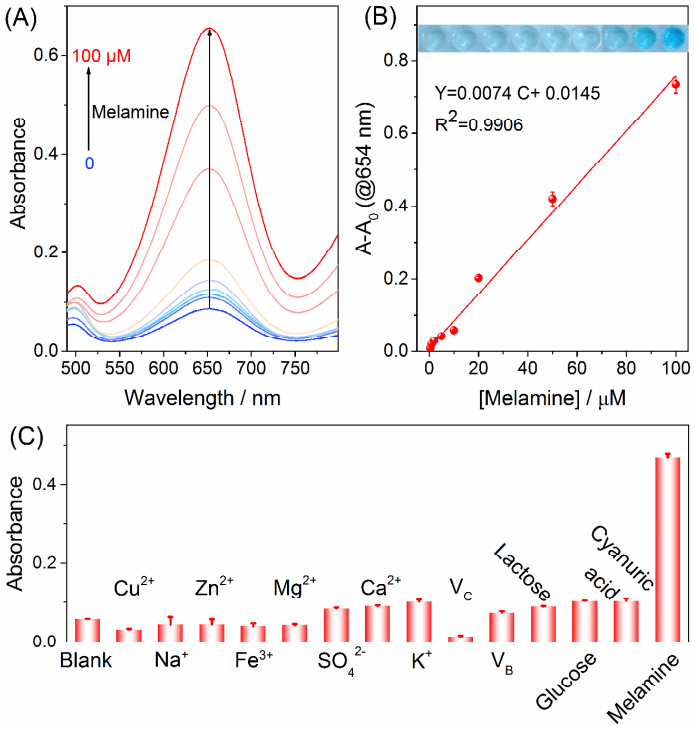

Figure 5 Analytical performance of the proposed assay for melamine detection: (A) absorption spectra of TMB in the presence of incrased amounts of melamine; (B) plot of the absorbance of TMB versus the concentration of melamine, the inset shows the corresponding photos; and (C) selectivity of this assay for melamine detection against co-existing substances potentially existed in dairy products and cyanuric acid.

The selectivity of the proposed mealmine assay was tested against a series of

co-existing substances potentially existed in dairy products, including Cu^{2+}, Na^{+}, Zn^{2+}, Fe^{3+}, Mg^{2+}, SO_4^{2-}, Ca^{2+}, K^{+}, ascorbic acid (VC), vitamin B (VB), lactose, and glucose, and also structure analogue of mealmine, namely cyanuric acid.[40] As shown in Figure 5C, most of the common substances in dairy products and analogues of melamine exhibit negligible interferences at 500 μM level on the determination of 50 μM melamine. Clearly, such good selectivity originates from the selective recognition of melamine by thymine, i.e., stable triple hydrogen-bonding between melamine and thymine.[33]

It should be noted that Hg^{2+} can also stabilize the T-T mismatch (T-Hg-T).[41] Therefore, singlet oxygen may also be generated when replacing melamine with Hg^{2+}, i.e., Hg^{2+} is a potential interferent for melamine detection. As shown in Figure S10, although not as efficient as that of melamine, Hg^{2+} did induce photo-oxidation of TMB. Fortunately, the abundance of Hg^{2+} in milk-based samples is significantly lower than that of melamine, since melamine may be added artificially for increasing the nitrogen content, while Hg^{2+} has no such artificial origin.

Dairy milk products containing melamine are assimilated by human that can induce renal pathology and even death in babies and children.[40] The potential applications of the proposed melamine assay were verified for the detection of melamine in dairy products. As shown in Table 2, no melamine was detected in the pretreated milk and milk powder samples, and then the samples were analysed with a standard-addition method with adding certain amounts of melamine to the sample solutions. The quantitative spike-recoveries ranged from 94% to 106%, demonstrating

the potential application of the proposed dsDNA (T-M-T)-SG system for photocatalytic visual detection of melamine in real dairy milk products.

Table 2. Analytical Results of Dairy Product Samples with the Proposed Biosensor.

Sample	Spiked (μM)	This method (μM)	Recovery (%)
Pure milk-1	10	10.6 ± 0.4	105.7 ± 4.5
Pure milk-2	20	19.6 ± 0.6	98.2 ± 3.1
Pure milk-3	50	52.5 ± 0.4	105.1 ± 0.9
Milk powder-1	10	9.4 ± 0.4	94.3 ± 4.1
Milk powder-2	20	20.7 ± 0.2	103.5 ± 1.2
Milk powder-3	50	51.3 ± 1.2	102.7 ± 2.4

CONCLUSION

In summary, melamine-mediated formation of dsDNA was explored for DNA-controlled photosensitized generation of $^1O_2$. Due to the stable melamine-thymine complex, dsDNA was successfully formed from the full T-DNA in the presence of melamine. Such process could efficiently modulate the photosensitization performance of SG, resulting in increased generation of $^1O_2$. In combination with $^1O_2$-induced TMB oxidation, visual detection of melamine was achieved. In lighting of the versatility of various DNA switches and functional DNAs, as well as the various schemes of DNA-controlled photosensitization, such integration will be promising in future sensor developments and PDT applications.

ACKNOWLEDGEMENT

The authors gratefully acknowledge the financial support from the National Natural Science Foundation of China (No. 21522505) and the Youth Science Foundation of Sichuan Province (Grant 2016JQ0019).

Supporting Information Available: Additional information as noted in text. This material is available free of charge via the Internet at http://pubs.acs.org.

Notes

The authors declare no competing financial interest.

REFERENCE

(1) Ogilby, P. R. *Chem. Soc. Rev.* **2010**, *39*, 3181-3209.
(2) Lucky, S. S.; Soo, K. C.; Zhang, Y. *Chem. Rev.* **2015**, *115*, 1990-2042.
(3) Abrahamse, H.; Hamblin, M. R. *Biochem. J.* **2016**, *473*, 347-364.
(4) Liu, C.; Kong, D.; Hsu, P.-C.; Yuan, H.; Lee, H.-W.; Liu, Y.; Wang, H.; Wang, S.; Yan, K.; Lin, D.; Maraccini, P. A.; Parker, K. M.; Boehm, A. B.; Cui, Y. *Nat. Nanotechnol.* **2016**, *11*, 1098-1104.
(5) Courtney, C. M.; Goodman, S. M.; McDaniel, J. A.; Madinger, N. E.; Chatterjee, A.; Nagpal, P. *Nat. Mater.* **2016**, *15*, 529-534.
(6) Long, R.; Mao, K. K.; Ye, X. D.; Yan, W. S.; Huang, Y. B.; Wang, J. Y.; Fu, Y.; Wang, X. S.; Wu, X. J.; Xie, Y.; Xiong, Y. J. *J. Am. Chem. Soc.* **2013**, *135*, 3200-3207.
(7) Dahal, E.; Curtiss, J.; Subedi, D.; Chen, G.; Houston, J. P.; Smirnov, S. *ACS Appl. Mater. Interfaces* **2015**, *7*, 9364-9371.
(8) Zhang, X. F.; Huang, C. P.; Xu, S. X.; Chen, J. B.; Zeng, Y.; Wu, P.; Hou, X. D. *Chem. Commun.* **2015**, *51*, 14465-14468.
(9) Tørring, T.; Helmig, S.; Ogilby, P. R.; Gothelf, K. V. *Acc. Chem. Res.* **2014**, *47*, 1799-1806.
(10) Cló, E.; Snyder, J. W.; Ogilby, P. R.; Gothelf, K. V. *ChemBioChem* **2007**, *8*, 475-481.
(11) Cló, E.; Snyder, J. W.; Voigt, N. V.; Ogilby, P. R.; Gothelf, K. V. *J. Am. Chem. Soc.* **2006**, *128*, 4200-4201.
(12) Tang, Z. W.; Zhu, Z.; Mallikaratchy, P.; Yang, R. H.; Sefah, K.; Tan, W. H. *Chem.-Asian J.* **2010**, *5*, 783-786.
(13) Zhu, Z.; Tang, Z. W.; Phillips, J. A.; Yang, R. H.; Wang, H.; Tan, W. H. *J. Am. Chem. Soc.* **2008**, *130*, 10856-10857.
(14) Han, D.; Zhu, G.; Wu, C.; Zhu, Z.; Chen, T.; Zhang, X.; Tan, W. *ACS Nano* **2013**, *7*, 2312-2319.
(15) Chen, J.; Lovell, J. F.; Lo, P. C.; Stefflova, K.; Niedre, M.; Wilson, B. C.; Zheng, G. *Photochem. Photobiol. Sci.* **2008**, *7*, 775-781.
(16) Hirakawa, K.; Hirano, T.; Nishimura, Y.; Arai, T.; Nosaka, Y. *J. Phys. Chem. B* **2012**, *116*,

3037-44.
(17) Hirakawa, K.; Hirano, T. *Photochem. Photobiol.* **2008**, *84*, 202-208.
(18) Hirakawa, K.; Harada, M.; Okazaki, S.; Nosaka, Y. *Chem. Commun.* **2012**, *48*, 4770-4772.
(19) Dumont, E.; Monari, A. *J. Phys. Chem. B* **2015**, *119*, 410-419.
(20) Tørring, T.; Toftegaard, R.; Arnbjerg, J.; Ogilby, P. R.; Gothelf, K. V. *Angew. Chem. Int. Ed.* **2010**, *49*, 7923-7925.
(21) Chen, C. E.; Zhou, L.; Geng, J.; Ren, J. S.; Qu, X. G. *Small* **2013**, *9*, 2793-2800.
(22) Wang, F.; Liu, X. Q.; Willner, I. *Angew. Chem. Int. Ed.* **2015**, *54*, 1098-1129.
(23) Stulz, E.; Clever, G.; Shionoya, M.; Mao, C. D. *Chem. Soc. Rev.* **2011**, *40*, 5633-5635.
(24) Ai, K.; Liu, Y.; Lu, L. *J. Am. Chem. Soc.* **2009**, *131*, 9496-9497.
(25) Huang, H.; Li, L.; Zhou, G.; Liu, Z.; Ma, Q.; Feng, Y.; Zeng, G.; Tinnefeld, P.; He, Z. *Talanta* **2011**, *85*, 1013-1019.
(26) Wang, G. L.; Jiao, H. J.; Zhu, X. Y.; Dong, Y. M.; Li, Z. J. *Talanta* **2012**, *93*, 398-403.
(27) Filigenzi, M. S.; Tor, E. R.; Poppenga, R. H.; Aston, L. A.; Puschner, B. *Rapid Commun. Mass Spectrom.* **2007**, *21*, 4027-4032.
(28) Zhu, L.; Gamez, G.; Chen, H.; Chingin, K.; Zenobi, R. *Chem. Commun.* **2009**, 559-561.
(29) Wang, Y.; Sun, Q.; Zhu, L.; Zhang, J.; Wang, F.; Lu, L.; Yu, H.; Xu, Z.; Zhang, W. *Chem. Commun.* **2015**, *51*, 7958-61.
(30) Lee, J.; Jeong Jeong, E.; Kim, J. *Chem. Commun.* **2011**, *47*, 358-60.
(31) Han, S.; Zhu, S.; Liu, Z.; Hu, L.; Parveen, S.; Xu, G. *Biosens. Bioelectron.* **2012**, *36*, 267-70.
(32) Wang, Y.; Zhang, J.; Zhu, L.; Lu, L.; Feng, C.; Wang, F.; Xu, Z.; Zhang, W. *Analyst* **2015**, *140*, 7508-12.
(33) Zeng, Y.; Pratumyot, Y.; Piao, X.; Bong, D. *J. Am. Chem. Soc.* **2012**, *134*, 832-835.
(34) Zipper, H.; Brunner, H.; Bernhagen, J.; Vitzthum, F. *Nucleic Acids Res.* **2004**, *32*, e103-e103.
(35) Dragan, A. I.; Pavlovic, R.; McGivney, J. B.; Casas-Finet, J. R.; Bishop, E. S.; Strouse, R. J.; Schenerman, M. A.; Geddes, C. D. *J. Fluoresc.* **2012**, *22*, 1189-1199.
(36) Dave, N.; Chan, M. Y.; Huang, P. J. J.; Smith, B. D.; Liu, J. W. *J. Am. Chem. Soc.* **2010**, *132*, 12668-12673.
(37) Miyake, Y.; Togashi, H.; Tashiro, M.; Yamaguchi, H.; Oda, S.; Kudo, M.; Tanaka, Y.; Kondo, Y.; Sawa, R.; Fujimoto, T.; Machinami, T.; Ono, A. *J. Am. Chem. Soc.* **2006**, *128*, 2172-2173.
(38) Chung, Y. J.; Lee, B. I.; Ko, J. W.; Park, C. B. *Adv. Healthc. Mater.* **2016**, *5*, 1560-1565.
(39) Long, R.; Huang, H.; Li, Y. P.; Song, L.; Xiong, Y. J. *Adv. Mater.* **2015**, *27*, 7025-7042.
(40) Li, Y.; Xu, J.; Sun, C. *RSC Adv.* **2015**, *5*, 1125-1147.
(41) Huang, J.; Gao, X.; Jia, J.; Kim, J.-K.; Li, Z. *Anal. Chem.* **2014**, *86*, 3209-3215.

For TOC only

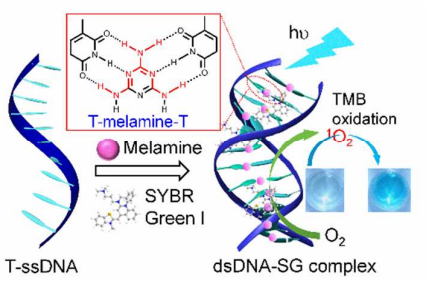
hυ
T-melamine-T
Melamine
SYBR
Green I
TMB
oxidation
$^1O_2$
O_2
T-ssDNA
dsDNA-SG complex